Gene exchange drives the ecological success of a multi-host bacterial pathogen

Emily J. Richardson[1,15,16], Rodrigo Bacigalupe[1,15], Ewan M. Harrison[2,15], Lucy A. Weinert[3,15], Samantha Lycett[1], Manouk Vrieling[1], Kirsty Robb[4], Paul A.Hoskisson[4], Matthew TG Holden[5], Edward J. Feil[6], Gavin K. Paterson[7], Steven YC Tong[8], Adebayo Shittu[9], Willem van Wamel[10], David M. Aanensen[11], Julian Parkhill[12], Sharon J. Peacock[13], Jukka Corander[12,14], Mark Holmes[3], and J. Ross Fitzgerald[1]*

[1]The Roslin Institute, University of Edinburgh, Easter Bush Campus, Edinburgh EH25 9RG, UK; [2]Dept. of Medicine, University of Cambridge, Addenbrooke's Hospital, Hills Road, Cambridge CB20QQ, UK; [3]Dept. of Veterinary Medicine, University of Cambridge, Madingley Rd, Cambridge CB30ES, UK; [4]University of Strathclyde, Glasgow; [5]School of Medicine, University of St. Andrews, St Andrews KY16 9TF, UK; [6]Milner Centre for Evolution, 4 South, University of Bath, Claverton Down, Bath BA2 7AY, UK; [7]Royal (Dick) School of Veterinary Studies, University of Edinburgh, Easter Bush Campus, Edinburgh EH25 9RG; [8]Victorian Infectious Disease Service, The Royal Melbourne Hospital, and The University of Melbourne, at the Peter Doherty Institute for Infection and Immunity, Victoria, Australia and Menzies School of Health Research, Darwin, Australia; [9]Department of Microbiology, Obafemi Awolowo University, Ile-Ife, Nigeria; [10]Department of Medical Microbiology and Infectious Diseases, Erasmus MC, Rotterdam, Netherlands; [11]Centre for Genomic Pathogen Surveillance, Wellcome Genome Campus, Cambridgeshire, CB10 1QY, UK and Dept. Infectious Disease Epidemiology, Imperial College London, W2 1PG,UK; [12]Wellcome Trust Sanger Institute, Hinxton; [13]London School of Hygiene and Tropical Medicine, London; [14]Helsinki Institute for Information Technology, Department of Mathematics and Statistics, University of Helsinki, Helsinki, Finland and Department of Biostatistics, University of Oslo, Norway.

[15]These authors contributed equally

[16]Current address: Institute of Microbiology and Infection, University of Birmingham, Edgbaston, Birmingham, B15 2TT, UK

Running title: *Staphylococcus aureus* host adaptation genome evolution

Keywords: Evolution; *Staphylococcus aureus*; host-species; adaptation; genomics

*Corresponding author: J. Ross Fitzgerald, The Roslin Institute, University of Edinburgh
e-mail: Ross.Fitzgerald@ed.ac.uk
Phone: +44 (0)131 6519235

Abstract

The capacity for some pathogens to jump into different host-species populations is a major threat to public health and food security. *Staphylococcus aureus* is a multi-host bacterial pathogen responsible for important human and livestock diseases. Here, using a population genomic approach we identify humans as a major hub for ancient and recent *S. aureus* host-switch events linked to the emergence of endemic livestock strains, and cows as the main animal reservoir for the emergence of human epidemic clones. Such host-species transitions are associated with horizontal acquisition of genetic elements from host-specific gene pools conferring traits required for survival in the new host-niche. Importantly, genes associated with antimicrobial resistance are unevenly distributed among human and animal hosts reflecting distinct antibiotic usage practices in medicine and agriculture. In addition to gene acquisition, genetic diversification has occurred in pathways associated with nutrient acquisition, implying metabolic remodeling after a host-switch in response to distinct nutrient availability. For example, *S. aureus* from dairy cattle exhibit enhanced utilization of lactose, a major source of carbohydrate in bovine milk. Overall, our findings highlight the influence of human activities on the multi-host ecology of a major bacterial pathogen, underpinned by horizontal gene transfer and core genome diversification.

Introduction

Many bacterial pathogens are host specialists that co-evolve with a single host-species. However, the capacity to switch host species can provide opportunities for expansion into new host populations. The domestication of animals in the Neolithic period (10,000-2,000 BC approximately) and the more recent intensification of livestock farming provided increased opportunities for the movement of bacterial pathogens between humans and animals[1]. Of note, the majority of emerging human infectious diseases have been traced to an animal origin[2]. *Staphylococcus aureus* is associated with a wide spectrum of diseases in humans and strains of both methicillin-sensitive (MSSA) and methicillin-resistant *S. aureus* (MRSA) are common causes of nosocomial and community-acquired infection[3,4]. In addition, *S. aureus* causes an array of infections of livestock that are a major burden on the agricultural industry, including mastitis in cows, sheep and goats [5,6], septicemia and skeletal infections in commercial broiler chickens[7], exudative epidermitis in pigs[8] and skin abscesses and mastitis in rabbits[9].

S. aureus has a clonal population structure defined by a relatively low level of recombination, comprised of lineages that have single or multiple host-tropisms[10-12]. Inter-host species transmission can be of critical public health importance, as exemplified by the livestock-associated methicillin-resistant clonal complex (CC) 398, which is associated with pigs and other livestock, but can cause zoonotic infections of pig-farmers and their contacts[13,14]. Previous work employed multi-locus sequence typing (MLST) to provide evidence for the occurrence of host-jump events from humans

leading to the emergence of *S. aureus* clones in livestock populations[11,12]. More recently, whole genome sequencing has been employed to investigate the evolution of individual clones, providing insights into the emergence, transmission and acquisition of antibiotic resistance in hospital, community, and agricultural settings[13,15-17]. In addition, a role for specific mobile genetic elements (MGEs) and core gene mutations in the host-adaptation of *S. aureus* has been identified [9,18,19]. For example, the major porcine and avian clones of *S. aureus* likely originated in humans and the host-jumps were associated with acquisition of MGE not found among human isolates [13,18]. Similarly, the major *S. aureus* clone associated with sheep and goats evolved through a combination of gene acquisition, and allelic diversification including loss of gene function[20]. Furthermore, several studies have reported the host-specific functional activity of *S. aureus* effectors such as leucocidins, superantigens, and the von Willebrand factor-binding protein [21-26]. In addition, it was demonstrated that for *S. aureus* strains associated with natural infections of rabbits, a single mutation was responsible for conferring infectivity to the progenitor strain found in human populations[9]. Taken together, these studies highlight the capacity for bacteria to undergo host-switching events and adapt to different species by multiple evolutionary genetic and functional mechanisms. However, a large-scale, genome-based analysis of the evolutionary history of *S. aureus* in the context of its host ecology is lacking, and the scale and molecular basis of host-switching events remains poorly understood.

Here, we carry out a population genomic analysis of over 800 *S. aureus* isolates selected to represent the known breadth of host-species diversity in order to provide a

high-resolution picture of the dynamics of *S. aureus* in the context of its host. The data reveal the impact of human activities such as domestication and the use of antibiotics in medicine and agriculture on the recent evolution of *S. aureus*, and identify the key evolutionary processes underpinning its multi-host species ecology.

Results

Extensive host-switching events define the evolutionary history of *S. aureus*.

We selected *S. aureus* strains to represent the breadth of the known clonal, geographic, and host-species diversity (Isolate selection details in Methods section). Overall, we included 800 isolates representative of 43 different host species, 77 clonal complexes (CCs), isolated in 50 different countries across 5 continents (Supplementary Figure 1-3; Supplementary Table 1). Among the 800 isolates, a total of 115,149 SNPs were identified in a core genome of 711,562 bp and used for reconstruction of the maximum-likelihood (ML) phylogeny for the *S. aureus* species (Fig. 1). The *S. aureus* species tree indicates the existence of highly divergent clades representative of the recently-described *Staphylococcus argenteus* and *Staphylococcus schweitzeri* species which belong to the extended *S. aureus*-related complex (Fig. 1a)[27]. *S. argenteus,* an emerging cause of human clinical infection[28], is more closely related to bat and monkey isolates than to other human *S. aureus* sequence types (STs), consistent with a possible non-human evolutionary origin for *S. argenteus*. Removal of isolates from the divergent clades resulted in a phylogeny of 783 isolates that segregated according to clonal complexes defined by MLST (Fig. 1b). The phylogeny indicates the broad diversity of isolates of human origin with expansion of several successful epidemic hospital and community-associated clones including CC22, CC30, and ST45, as previously described[29] (Fig. 1). Animal isolates are typically found in discrete host-specific clades interspersed among human lineages, consistent with ancient and recent host-switching events across the phylogenetic tree (Fig. 1). In order to examine the frequency and timing of host-switching events during the evolution of *S. aureus*, we

151 employed Bayesian evolutionary analysis by sampling trees (BEAST) using substitution
152 rates from published datasets (Fig. 2; Supplementary Table 2). We estimated the
153 number of cross-species transmissions for 10 major host categories (Supplementary
154 Table 3, Supplementary Figures 2-5) using BEAST with Markov Jumps[30]. In order to
155 reduce bias caused by the larger numbers of sequences from human and cow hosts
156 compared to the other host types we used 10 stratified subsamples containing 252
157 sequences each, designed to maintain geographic, host-type and temporal diversity
158 while reducing over-representation. To assess the robustness of the main analysis, we
159 performed additional analyses as outlined in Supplementary Material (Supplementary
160 Notes; Supplementary Figures 4-11; Supplementary Tables 4-5), that included 'severe
161 balanced' subsamples of 97 taxa each containing 18-20 taxa of 5 host-types, and
162 ancestral state and host-jumps using the BASTA approximation to the structured
163 coalescent[31]. However, we had difficulty in getting BASTA to run and converge possibly
164 due to its assumptions about the structure of the data and numerical instability. Each
165 subsampled sequence set was analyzed separately within BEAST and resulted in a
166 collection of posterior trees per dataset (Supplementary Figures 6-10). In each case, the
167 analysis revealed extensive host-switching events that occurred over a time-frame
168 spanning several thousand years up to the present decade (Fig. 2a).
169
170 Our analysis identifies humans as a major donor with host-jumps identified from
171 humans into all other host-species groups examined (Fig. 2b, Supplementary Figure 4).
172 The most common recipient for *S. aureus* jumps from humans was cows with a median
173 of 14 jumps (HPD 3-22) between the years -2000 and 2012. Cows also represented a
174 major donor for host-switching events back into humans (n=10; HPD 2-26). In addition,

175 there were numerous *S. aureus* host-switches among ruminants, particularly between
176 cattle and goats in both directions and into sheep. However, host jumps from sheep into
177 other species are rare and not strongly supported by our analyses suggesting that
178 although a common host for *S. aureus* [5], sheep do not represent a major reservoir for
179 the spread of *S. aureus* to other animals.
180
181 **Host-specific accessory gene pools promote adaptive evolution after host-**
182 **switching events.** In order to investigate the distribution of MGEs on a population level
183 across human and animal isolates, we employed a pangenome-wide association
184 analysis approach to identify genes that were enriched among isolates from specific
185 host-species. First, to account for phylogeny we removed genes identified among all
186 strains within clonal complexes associated with multiple host-species (lineage-
187 dependent genes). Network analysis indicated a remarkable correlation between
188 accessory genome and host-species revealing that diverse clonal complexes can share
189 highly similar accessory genomes that are specific for birds, pigs or horses,
190 respectively. This strongly points to the existence of a host-specific gene pool required
191 for *S. aureus* host-adaptation. Although accessory genomes of *S. aureus* obtained from
192 humans, and from cows, sheep and goats also tended to cluster together in a host-
193 specific manner, there was greater diversity in gene content (Fig. 3). This may reflect
194 the existence of multiple cryptic niches that exist within a single host-species such as
195 those proposed previously for *Campylobacter jejuni* [32]. We note the existence of a small
196 number of clusters made of isolates from multiple host-species. The existence of these
197 clusters suggests that some accessory gene combinations may confer a more

198 generalist host tropism with the capacity to infect multiple host-species. Alternatively,
199 insufficient time may have passed since the host-transition event for loss of dispensable
200 MGE to occur. Of note, antibiotic resistance gene determinants influenced the clustering
201 of equine and pig isolates suggesting a role for acquisition of resistance in host-
202 adaptation (Supplementary Figure 12).
203
204 Further examination of the impact of the accessory genome on successful host-
205 switching events was carried out by identifying gene acquisition or loss events that
206 correlated with host-switching events identified on the phylogeny of *S. aureus*. A total of
207 36 distinct MGEs including predicted plasmids, transposons, *S. aureus* Pathogenicity
208 Islands (SaPIs) and prophages were identified to be associated with host-switch events
209 ($p< 0.0001$) (Fig. 4a, Supplementary Table 6). Several of the MGEs have previously
210 been identified and demonstrated to encode proteins with host-specific activity. For
211 example, the β-converting phage ϕSa3 encodes modulators of the human innate
212 immune response, and pathogenicity islands encode superantigens or von Willebrand
213 factor-binding proteins with ruminant-specific activity [19,33]. In addition, equine isolates
214 contain a phage encoding a novel equine allele of the staphylococcal inhibitor of
215 complement (*scn*) which also encodes the LukP/Q toxin, recently characterized to have
216 equine-specific activity[22,25]. However, numerous uncharacterized MGEs have been
217 identified in the current study to be linked to successful host-switch events providing
218 many novel avenues for characterizing the molecular basis of *S. aureus* host-adaptation
219 (Fig 4b). For example, in isolates from pigs, a putative novel plasmid linked to SCC*mec*
220 encoding resistance to heavy metal ions, a common supplement in pig-feed, was linked

to host-switching events from humans into pigs (Fig. 4b). Finally, several gene clusters encoding bacterocins were enriched in isolates from specific host-species ($p < 0.0001$) or were linked to host-switching events ($p<0.0001$), consistent with the need to compete with resident bacteria for survival (Supplementary Table 6). Taken together, these data suggest that successful host-switch events are associated with acquisition of MGEs from an accessory gene pool that exists in the recipient host-species, and/or loss of MGEs linked to the source species.

In order to investigate the potential origin of MGEs horizontally acquired after a host-switch event, we examined the codon usage bias of host-specific MGE, and found that MGEs enriched in pig isolates had significantly elevated %GC content and reduced codon adaptive index (CAI) indicative of a distinct genealogical origin (Supplementary Figures 13-15). Of note, an MGE found in pig isolates had highest BLASTn similarity to a putative pathogenicity island previously identified in the pig-associated zoonotic pathogen *Streptococcus suis* (GC content of ~41%) (Supplementary Table 6).

Both gain and loss of gene function are associated with *S. aureus* host-adaptation. Determination of the number of predicted functional genes in each *S. aureus* genome identified a significantly higher number of genes in bird strains compared to *S. aureus* from any other host-species (Supplementary Figures 16-17). In contrast, the number of pseudogenes per genome is significantly higher ($p<0.0001$-0.02) in ruminant strains compared to those from other host-species suggesting that the niche occupied by *S. aureus* in cows may provide stronger selection for loss of gene

function compared to the niches for *S. aureus* in birds and pigs. Numerous pseudogenes associated with transport of nutrients in *S. aureus* including carbohydrates, are over-represented in ruminant isolates implying metabolic remodeling in response to distinct nutrient availabilities in the bovine niche (Supplementary Table 8).

Refinement of host adaptation involves modification of biological pathways in response to nutrient availability. In addition to accessory genes, adaptive mutations in the core genome may be selected for in response to environmental changes such as antibiotic exposure or a switch in host-species [9,34]. In order to examine the impact of host-species on diversification of the *S. aureus* core genome, we identified groups of related isolates (e.g. within CCs or STs) associated with a specific host-species for genome-wide analysis of positive selection (Supplementary Table 9; Supplementary Figure 18). Positive selection was identified across all host-associated groups examined, with an average of 68 genes (33 to 129) representing approximately 2.7% (1.3% to 5.1%) of a clade-specific core genome (Supplementary Table 10). A limited number of genes were under diversifying selection across multiple host species, including several that encode membrane proteins, lipoproteins and a protein involved in biofilm formation. Some genes were identified as undergoing positive selection in distinct lineages that were associated with the same host-species (mostly human), suggesting strong selective pressure leading to convergent evolution. However, for the most part, our analysis detected distinct sets of genes under positive selection in different lineages, suggesting that signatures of host-adaptation are dependent on the

genetic background of the strain, and that host-adaptation can occur via multiple trajectories involving modification of distinct pathways.

We predicted functional categories of genes under positive selection and the biological pathways affected revealing several functional groups that were enriched for positively selected genes independently of the host species including genes linked to pathogenesis, immune evasion and maintenance of MGEs ((Supplementary Table 11; Supplementary Figure 19). However, the majority of the functional categories were host-species dependent, consistent with distinct mechanisms underpinning adaptation to different host-species (Supplementary Table 11; summarized Fig. 5). In particular, biological pathways associated with amino acid metabolism and iron acquisition were under positive selection in several host-species suggesting diversification in response to distinct nutrient availability in different host niches. In addition, genes associated with transport and metabolism of carbohydrates demonstrated signatures of positive selection in *S. aureus* clones from humans and cows (Fig. 5).

Bovine *S. aureus* strains utilize lactose with higher efficiency compared to human or avian strains. Considering the signatures of positive selection identified among pathways associated with carbohydrate and amino acid metabolism, we investigated differences in growth phenotype of selected host-specific *S. aureus* strains using a metabolic phenotype microarray (Biolog), and observed preliminary strain-dependent differences in growth that were influenced by the availability of specific amino acids or carbohydrates. For example, *S. aureus* strains from cows had higher relative growth in

290 the presence of lactose, the primary disaccharide available in bovine milk. The genome-
291 wide positive selection analysis indicated that in bovine strains, genes associated with
292 the functional category of transport of disaccharides and oligosaccharides were
293 impacted by positive selection. To further investigate this, we carried out phenotypic
294 analysis of *S. aureus* strains from bovine, human and avian host- species of different
295 clonal complexes when grown in the presence of lactose (Fig. 5e). As lactic acid is
296 produced by *S. aureus* as a by-product of fermentation, we measured pH levels in
297 culture media containing lactose and identified a decrease in pH levels for bovine *S.*
298 *aureus* clones in comparison to human or avian clones, consistent with increased
299 efficiency of fermentation of lactose (Fig. 5f). These data support the concept that *S.*
300 *aureus* undergoes genetic diversification in response to the nutrients that differ in
301 availability in different niches.
302
303 **Resistance to antimicrobials differs among human and pig *S. aureus*.** Our
304 understanding of the relative contribution of the use of antibiotics in human medicine
305 and agriculture to the emergence of antibiotic resistance is very limited. To address this
306 question for the model human and animal pathogen *S. aureus*, we examined the
307 distribution of antibiotic, antiseptic and heavy metal-ion resistance determinants among
308 human and livestock isolates, and then accounted for phylogenetic relatedness for
309 resistance to different classes of antibiotic (Supplementary Table 12). An array of
310 resistance determinants were significantly enriched in human, ruminant, and pig
311 isolates, respectively, but not among avian isolates, consistent with a limited role for the
312 poultry industry in the emergence of antibiotic resistance in *S. aureus*.(Fig. 6; Table

S12). When testing for phylogenetic independence, we aimed to maximize statistical power by including all gene determinants into groups specific for each class of antimicrobial, and also examined selected individual determinants *str* and *sdrM*. The analysis indicated that resistance to streptomycin, antiseptics, and tetracyclines were all significantly associated with pig isolates, whereas *sdrM* was enriched in human isolates. However, fluoroquinolone and heavy metal ion resistance did not correlate with hosts after correction for phylogeny implying that expansion of specific clones has contributed to the high frequency of those resistance determinants among human and pig hosts, respectively. Taken together, these data demonstrate that resistance to specific classes of antimicrobial in *S. aureus* is host species-dependent providing evidence for distinct antibiotic selective pressures in humans and livestock. Of note tetracyclines, and aminoglycosides (such as streptomycin) are used in much higher amounts in farmed animals compared to human medicine [35]. Zoonotic transmission of *S. aureus* is a relatively common occurrence for some clones, particularly between pigs and humans in the case of CC398, providing a route for the transmission of resistant strains and associated resistance determinants to humans[36].

Discussion

Many new pathogens emerge following zoonotic or anthroponotic events providing the opportunity for spread within a new host population[2]. *S. aureus* is considered a generalist bacterial species, capable of colonizing a wide range of hosts[5]. However, the species is composed of distinct sub-lineages that are commonly associated with

particular hosts or host groups[10,14]. Accordingly, *S. aureus* represents an excellent model to explore the dynamics of a bacterial pathogen at the human-animal interface. Here, we demonstrate that the segregated host-specialism of *S. aureus* arose via multiple cross-species transmission events that occurred over the last 5,000-6,000 years, leading to the emergence of successful endemic and epidemic clones circulating in distinct host-species populations. We identify humans as a major reservoir for the spread of *S. aureus* to livestock, reflecting the role of humans in domestication of animals, and subsequent opportunities for cross-species transmission events consistent with analysis using MLST[12]. Importantly, we also identify cows as the main animal source for the emergence of *S. aureus* clones that are epidemic in human populations consistent with a previous study that identified a bovine origin for emergent CC97 clones causing human infections across multiple continents[17].

The identification of combinations of MGEs that are associated with specific host-species and linked to host-switching events provides compelling evidence for the key role of horizontal gene acquisition in the adaptation of *S. aureus* to their hosts. While several MGEs have been identified to be associated with host-specific clones[18,19,22,24], our species-wide analysis reveals combinations of MGEs linked to specific host species providing many new avenues for investigating mechanisms of bacterial host-adaptation. Overall, the data suggest that host-specific accessory gene pools presumably present in the microbiota of the new host-species promote the host-adaptive evolution of *S. aureus*.

In addition to gene acquisition associated with host-switch events, we identified evidence of adaptive evolution in the core genome consistent with host-specific selective pressure driving the diversification of biological pathways that are involved in survival or transmission. Furthermore, in some cases, distinct pathways were under positive selective pressure in different clones associated with the same host-species, implying that multiple distinct pathways may mediate host-adaptation depending on the genetic background of the strain. In particular, pathways linked to carbohydrate transport exhibited signatures of host-adaptation and phenotypic analysis revealed enhanced utilization by bovine S. aureus clones of the disaccharide lactose, the major carbohydrate available in bovine milk.

These findings inform a model of *S. aureus* host-adaptation in which acquisition of a specific set of MGEs occur rapidly after a host-switch event (although we can't rule out this could occur prior to the jump in some cases), conferring the capacity for survival in the new host, largely through targeting of the innate immune response via bacterial effectors such as leukocidins, superantigens and other immune-modulators. Other MGEs confer resistance to antibiotics and heavy metal ions allowing survival under strong anti-microbial selective pressures. Subsequently, positive selection acts on the core genome via point mutation and/or recombination [37] causing allelic variation and loss of gene function that results in modification of metabolism in response to distinct nutrient availability.

Our findings suggest that since human-driven domestication, interactions with livestock have provided opportunities for numerous successful host-switch events between humans and livestock hosts. Further, industrialization of agriculture including use of antibiotics and feed supplements in intensive farming have directly influenced the evolution of *S. aureus* clones resulting in the emergence of resistance in response to distinct antibiotic selective pressures in human medicine and agriculture[18,38]. These data support the idea that surveillance could play a critical role in the early identification of emerging clones that have jumped host.

Taken together, our data provide a high-resolution view of the capacity for a model multi-host pathogen to undergo radical changes in host ecology by genetic adaptation. Investigation into the functional basis of these genetic changes will reveal key host-pathogen interactions that could be targeted for novel therapies. Further, the identification of the common routes for *S. aureus* livestock-human host-species switches and distinct types of antimicrobial resistance in humans and livestock species could inform the design of more effective farm security and antibiotic treatment practices to limit the emergence of new resistant clones. These findings will be relevant to other major bacterial pathogens with the capacity to spread between livestock and humans.

Methods

Isolate selection. For selection of isolates, the literature was reviewed (date: November 2013) and all available *S. aureus* strains associated with animals and

404 humans for which genomes had been determined were identified. We aimed to include
405 isolates to represent the breadth of clonal complexes, host-species diversity,
406 geographical locations and as wide a temporal scale as possible (Supplementary
407 Tables 1-3). Publicly available sequences were selected as follows; 74 reference
408 genomes, 302 from the EARSS project[29], and 252 from other published studies of the
409 authors (Supplementary Table 1). Furthermore, to be as representative of the known *S.*
410 *aureus* host, clonal, and geographic diversity as possible we selected an additional 172
411 isolates for whole genome sequencing (Supplementary Table 1). Our dataset is biased
412 towards human isolates which represent approximately 60% of the total with 40%
413 approximately from animal sources. This reflects that fact that much of the known
414 diversity of the *S. aureus* species is of human origin[12], and also that fewer number of
415 isolates that have been obtained from animals. Given the predominant European origin
416 of the animal isolates (due to the contemporary interest in animal *S. aureus* in Europe),
417 we chose to enrich the number of human isolates with the EARSS collection
418 representative of the diversity of invasive *S. aureus* circulating among humans in
419 Europe in 2006[29]. Accordingly, there is a European bias to the sample dataset and we
420 can't rule out that we have under-sampled the *S. aureus* diversity that exists in other
421 parts of the world. Nonetheless, our dataset contained isolates from 50 different
422 countries across 5 continents and many sequence types are widely distributed on an
423 intercontinental scale. In addition, our dataset includes isolates from the years 1930 to
424 2014, although the majority have been isolated since 2005 reflecting the greater
425 availability of recent clinical isolates (particularly from animals). It should therefore also
426 be considered that the dataset is biased towards contemporary *S. aureus* and that older

lineages that are now less abundant or extinct may not be represented in our dataset. In order to partially address the uneven distributions of isolates by host, space and time, where appropriate, we have carried out experimental replicates based on severe subsampling of the dataset that provide more evenly distributed groups. In addition, we have drawn conclusions that are consistent across subsampled data and, when appropriate, multiple different analytic approaches. Overall, we included 800 isolates representative of 43 different host species and 77 clonal complexes (CCs), isolated in 50 different countries across 5 continents (Supplementary Table 1). All sequences and associated metadata have been uploaded to Microreact a publicly accessible database that allows visualization and analysis of the data https://microreact.org/project/shacdata [39].

Sequencing, genome assemblies, variant calling and phylogenetic reconstruction. For the current study, bacterial DNA was extracted and sequenced using Illumina HiSeq2000 with 100-cycle paired-end runs at the Wellcome Trust Sanger Institute or Illumina HiSeq2000 at Edinburgh Genomics. The nucleotide sequence data were submitted to the European Nucleotide Archive (ENA) (www.ebi.ac.uk/ena) with the accession numbers listed in Supplementary Table 1. Completed genomes downloaded from the NCBI database were converted into pseudo-fastq files using Wgsim (https://github.com/lh3/wgsim). For each isolate the sequence reads were used to create multiple assemblies using VelvetOptimiser v2.2.5[40] and Velvet v1.2[41]. The assemblies were improved by scaffolding the best N50 and contigs using SSPACE[42] and sequence gaps filled using GapFiller[43]. Isolates were excluded from the analysis for

450 the following reasons that are indicative of contamination or poor quality sequence data;
451 a large number of contigs and a large number of 'N's in the assemblies or large genome
452 size (>2.9 Mb). Sequence types were determined from the assemblies using MLST
453 check (https://github.com/sanger-pathogens/mlst_check), which was used to compare
454 the assembled genomes against the MLST database for *S. aureus*
455 (http://pubmlst.org/saureus/). Sequence reads were mapped to a relevant reference
456 genome (European Nucleotide Archive (ENA) ST425 (strain LGA251, accession
457 number FR821779), using SMALT (http://www.sanger.ac.uk/science/tools/smalt-0)
458 following the default settings to identify single nucleotide polymorphisms (SNPs).
459 Consensus sequences were obtained using samtools and concatenated into core
460 genome alignments[44]. SNPs located in mobile genetic elements were removed from the
461 alignments and a maximum likelihood tree was constructed using RAxML following
462 default settings and 1000 bootstrap replicates[45].
463
464 **Time scaled trees and estimation of the number of host jumps**. Time scaled trees
465 were generated using BEAST 1.8.2[46]. All isolates with unknown date, unknown host
466 species or unknown geographical location were removed in addition to the diverse
467 BAPs groups 12 and 14 leaving a total of 696 isolates. Sites determined to be affected
468 by recombination from the BNG analysis of the individual BAPs groups, were coded as
469 missing data. Since missing data can effect phylogenetic inference and contribute to
470 heavy likelihood calculations, sites that had more than one missing state in the
471 alignment (either from missing mapped reads or recombination) were excluded from
472 further analyses, leaving a total of 55,778 sites (4306 segregating sites).

To account for different evolutionary processes acting at synonymous and non-synonymous sites, RNA and noncoding sites, the evolutionary model was partitioned in to 1+2nd sites, 3rd sites, non-coding sites, and RNAs according to the reference strain LGA251. Pseudogenes were partitioned in to 1+2nd and 3rd sites with the rationale that they may be functional in other isolates. For overlapping reading frames, sites were assigned to the region of highest constraint (e.g. when coding and RNA, sites assigned as RNA, when 1st and 3rd, sites assigned as 1+2nd etc.). For all partitions, we used an HKY + Γ substitution model.

Dating. We treated all sequences as contemporaneous but assigned a median prior of 1.61 [0.604, 2.9] substitutions per site per million years on to 3rd positions, which are less likely to be subject to strong purifying selection (known to affect rates over different timescales). The prior comes from previous studies of *S. aureus* using tip dates on different strain types (Supplementary Table 3). An uncorrelated lognormal model of changes in substitution rate across different branches was employed. An initial MCMC run with this model was performed in BEAST v1.8.2[46] using Beagle[47] with two independent chains, removing the appropriate burnin and run for approximately 100,000,000 generations.

In addition, a 10 further subsampled datasets were produced that included only sequences from the 10 major host types. These were stratified subsamples containing 252 samples each, designed to maintain the host species, geographic and temporal diversity. The major hosts types are birds, cows, goats, carnivores, horses, humans,

rabbits, sheep, rodents and pigs. From these analyses, we subsampled an empirical distribution of 1000 trees post burnin which were used for all further BEAST analyses.

Markov Jump analysis. In order to reconstruct host transition events, we used an asymmetric discrete state phylogeographic analysis with Markov Jumps (REF: 51) applied to the 10 major host types with default priors. We employed the Markov jump analysis to estimate the posterior expectation of the number of host change events across the branches of the phylogeny[30], using posterior sets of 1000 time scaled trees from the initial BEAST analyses on the subsampled data sets. The trait models were used in an MCMC chain of 1,100,000 steps, sampling every 100 steps and discarding the first 10% as burn-in, leaving 10,000 trees annotated with the host information (i.e. approximately 10 model instances per tree of the original posterior set). Since biased sampling can lead to biased results when using these trait models, in addition to using the 10 stratified subsamples of 252 sequences each we performed additional analyses with host state randomization and using 100 bootstrapped maximum likelihood trees (RAxML) in place of the 1000 original BEAST trees (for the 10 stratified subsamples) To balance the numbers of isolates per host category further, we also created 10 ‘severe’ stratified subsamples containing 97 sequences each with 20 from Humans, Cows and Sheep+Goats combined and 19 and 18 from Birds and Pigs respectively. Necessarily in these severe subsamples it was not possible to maintain the full human and cattle diversity, although sequences from different geographic locations and years were chosen. We applied BEAST with Markov Jumps on these 5 host categories using: full joint inference of trees using sequences and traits together; trees using the sequences

only followed by the trait mapping as before; and the BASTA structured coalescent approximation [31].

Pseudogene analysis. Pseudogenes were predicted during the PROKKA annotation process[48]. Specifically, each protein in a genome was searched against UniProtKB (Swiss-Prot) using BLASTp[49] or UniProtKB (TrEMBL). If no significant hits were identified, proteins were examined for conserved motifs. Any proteins exhibited less than 95% coverage of their top hit were listed as potential pseudogenes. The region of the top hit that was not present in the protein sequence was then interrogated against all contigs using BLASTn[49]. Hits that were in the correct orientation and on the same contigs were accepted as pseudogenes and labelled according to their type (frameshift, stop codon, insertion). Proteins that were less 95% coverage of their top hit and on the edge of a contig with their counterpart on another contigs were not labelled as pseudogenes, rather CDS that have split due to the assembly breaking at this point.

The UniProt ID Mapping tool was used to assign Gene ontology (GO) terms to all pseudogenes by transferring the GO terms assigned to the closest reference (identified during the annotation process described above). GO was assigned to all non-pseudogenes (CDS features) using the same method and InterProScan[50]. The R package topGO[51] with Fisher's exact test was used to identify enriched GO terms whilst taking into account the GO hierarchy (the p-value was adjusted using Bonferroni correction).

Pan-genome association analysis. All genomes in this study were organised into a list of reference genomes followed by assembled contigs. The second genome in the list was aligned to the first genome using Nucmer[52] and any regions larger than 100 bp that did not map to the first genome were appended to the end of it to produce a pangenome representing the unique regions in the first two genomes. Each subsequent genome aligned to the combination of all unique regions from the previously aligned genomes in the list producing a pangenome that represents all of the nucleotide sequences of all genomes. All genes were organised into groups of orthologues using the bi-directional best hits algorithm in Get_homologues with a minimum coverage setting of 50% and minimum sequence identity setting of 80%[53]. The pangenome was used as the reference and the coding sequences (CDS) predicted in the annotations described previously were compared to all CDS within the pangenome. Features annotated as pseudogenes were excluded from this analysis. The Get_homologues compare_clusters perl script was used to create a pangenome matrix of all identified gene clusters against all genomes. All core gene clusters (clusters that contain genes from every genome) were removed from the pangenome matrix. Further to this all clusters that only contained genes from one genome or all genomes except one were removed. Furthermore, gene clusters that were found in all members of any STs associated with multiple host species were removed on the basis that they are not specific to a single host species. This has the effect of removing lineage-associated genes resulting in a set of gene clusters that are strain-dependent and largely independent of phylogeny. Hypergeometric testing was used to find over- and under-represented gene clusters for each host (the p-value was adjusted using Bonferroni

correction). All gene clusters were searched against the NCBI non-redundant nucleotide database using blastn to provide the most up to date annotation and to examine the likely bacterial species origin of each MGE.

A pairwise distance matrix was calculated from the pangenome matrix using the distmat function in EMBOSS[54]. The matrix was converted into a bidirectional graph with distance as the edge weight parameter. The graph was processed in BioLayout with an edge weight threshold of 0.5[55].

Identification of gene acquisitions or losses associated with host-switching events. The R package APE (Analysis of Phylogenetics and Evolution)[56] was used to fit a single discrete trait model and get the ancestral state of each node for each gene cluster against the phylogenetic tree. From this, a vector for every gene cluster was created with gene acquisition/loss events by comparing every child node in the tree to its parent node to determine if there was no change, a gene acquisition or a gene loss event. This was performed separately for each host type (i.e. human, ruminant, bird, horse and pig) to identify which nodes are associated with a host-switching event. All gene state vectors were compared to all host state vectors using a Fisher's exact test to show whether a gene loss/acquisition even is related to a host switch event. The p-values were adjusted using Bonferroni correction.

Codon usage bias analysis. The codon adaptation index is used to calculate codon usage bias by comparing the CAI of a gene against the codon usage table of a

reference set of genes. The codon usage table was calculated using the EMBOSS tool cusp[54]. For this study, the codon usage table was comprised of all genes that were not significantly over represented in a host or significantly associated with a host switch. The codon adaptation index (CAI) for all genes significantly over represented in a host and significantly associated with a host jump was calculated using the EMBOSS tool cai[54]. The codon adaptation index was also calculated using five random subsets of 50 genes as controls. A one-way ANOVA test was used to test whether there was a significant effect of host upon CAI. A Tukey HSD test was then applied to compare the CAIs between host species.

Distribution of antibiotic resistance genes analysis. Antimicrobial resistance genes were identified as described by Holden et al[15]. Resistance genes were identified by a combination of BlastN and mapping against assemblies and as previously described [57] and resistance SNPs identified by mapping against a pseudomolecule of genes with previously reported resistance-conferring mutations. Isolates were grouped into human isolates and all animals and them human, rabbits, companion animals (horses, dogs, cats), marine, pigs, primates, ruminants (goats, sheep, cows) and small mammals (rats, mice, other small mammals). The proportions of isolates with each resistance gene and ≥1 resistance conferring SNP for each antibiotic was compared to identify enrichment using a two-tailed Fishers Exact test with a Bonferroni correction for multiple testing. Determinates with a P value $<9.9 \times 10^{-5}$ were considered statistically significantly enriched. To examine whether the Fisher Exact tests of independence were robust when accounting for population structure, we tested whether resistance phenotypes and

610 host were correlated across the *S. aureus* phylogeny. We conducted these for
611 pig/human and ruminant/human since these were the only comparisons where
612 significant differences were observed according to the Fisher's exact test. In order to
613 maximise statistical power, we grouped all gene determinants into specific classes of
614 antimicrobial (e.g. Tetracycline-resistant if encoding any *tet* allele) and tested for
615 correlation with host species using the program BayesTraits[58] (using the posterior
616 sample of trees from our earlier BEAST analysis). We note that the correlated
617 evolutionary analysis may be overly conservative in cases where horizontal gene
618 transfer is rampant or homoplasies are high. BayesTraits uses a continuous-time
619 Markov model to estimate transition rates between the presence and absence of a gene
620 or SNP and between human and non-human hosts. We allowed the transition rates to
621 evolve in either a correlated fashion (where the rate of change in one trait depends on
622 the state found in the other trait) or independently. Posterior distributions of parameters
623 were estimated from up to 4 million iterations of the MCMC with default priors. After
624 discarding burn-in, the marginal likelihoods of the dependent and independent models
625 were obtained using the Akaike Information Criterion (AICM) estimated using the
626 methods-of-moment estimator in Tracer 1.6[59]
627
628 **Genome-wide positive selection analysis.** To identify genes under positive selection
629 in different host groups, we first identified lineages (STs or CCs) correlated with
630 particular hosts. As the power of the selection analysis is determined by the number of
631 isolates included, only clades with more than 10 isolates associated with a host were
632 considered. Based on these criteria, 15 CCs from four groups of hosts were analyzed: 9

633 for humans (CC30, CC5, CC59, CC15, CC12, ST239, ST8, CC22 and CC45), 3 for
634 ruminants (CC133, primarily associated with sheep and goats and the cows related
635 CC151 and CC97), 2 for birds (CC5 and CC385) and one for pigs (CC398)
636 (Supplementary Table 7). Although the CC398 clade also contained several human
637 isolates, these mostly represent spill-over events rather than an established association
638 so the CC398-human group was not included for the analysis. Given the variable
639 number of isolates of each CC-host group, in order to standardize the analysis while
640 preventing the underestimation of genes under positive selection, 10 isolates linked with
641 a host were analyzed at a time. Replicates or triplicates of different subsets of genomes
642 using sampling with replacement was carried out if the number of isolates for that
643 lineage was large enough. Next, we identified orthologous genes in each of these
644 groups using the algorithm OrthoMCL integrated in get_homologues (identity >70%,
645 similarity >75%, f50, e-value = 1e-5)[53]. Genes were considered orthologous if they were
646 present in at least 70% of the genomes. Since alignment of coding DNA sequences
647 may insert gaps in codons and produce frame-shifts, we aligned genes at the protein
648 level using MUSCLE 3.8.31[60] and translated these sequences back to DNA using
649 pal2nal v14[61]. Genes identified as inparalogous that turned out to be duplications were
650 kept for further analyses, otherwise discarded. For every alignment, recombination was
651 detected using the NSS, Max Chi and Phi tests included in PhiPack[62] and recombinant
652 genes removed from further analyses. For the gene clusters containing 10 isolates,
653 phylogenetic trees were extracted from the 783 isolates ML tree. For clusters with less
654 than 10 genomes, subtrees were produced from the general tree using the tree prune
655 function in ete2[63]. The DNA alignments and trees were used for PAML analysis[64]. We

656 employed the site evolution models of Codeml (M1a, M2a, M7, M8 and M8a) to perform
657 codon-by-codon analysis of dN/dS ratios (nonsynonymous to synonymous substitution,
658 ω) of genes and a likelihood ratio test (LRT) was used to determine significant
659 differences between nested models M1a-M2a, M7-M8, M8a-M8, where one accounts
660 for positive selection (alternative hypothesis) and the other specifies a neutral model
661 (null hypothesis). Statistic tests were assessed to a chi-square distribution with 2 and 1
662 degrees of freedom[64]. Bayes Empirical Bayes[65] was used to calculate the posterior
663 probabilities of amino acid sites under positive selection of proteins that had significant
664 LRTs. As independent replicates from similar CC/Host groups resulted in slightly
665 different genes positively selected, we used get_homologues to merge the core
666 genomes and genes selected for each group using same parameters as above. Genes
667 under positive selection were considered when they were in common for different
668 replicates with a p-value of 0.05 or were identified in different replicates with a stringent
669 p-value (0.05/number of genes per core genome).
670 To explore functional categories under positive selection we performed classification of
671 Clusters of Orthologous Groups (COGs), annotated Gene Ontology terms (GO) and
672 analysed metabolic pathways (KEGG). To assign COG terms, we performed BLASTp of
673 single representatives of the orthologous clusters against the prot2003-2014 database,
674 retrieving the top 5 hits to include alternative annotations. We mapped the gene IDS
675 obtained to the cog2003-2014.csv database from which the COGs were inferred.
676 Frequencies of COGs for positively selected genes in each CC-host were compared
677 with the average COG frequencies in the respective core genomes. GO annotations
678 were obtained by mapping the genes to the go_20151121-seqdb, uniprot_sprot and

679 uniprot_trembl databases using BLASTp. From these, the UniProtKB were mapped to
680 the gene_association_goa database and filtered by bacteria domain to obtain the GO
681 categories. To visualize and identify overrepresented GO categories of positively
682 selected genes in different hosts, we used BiNGO[66]. We identified overrepresented
683 categories using the hypergeometric test with the Benjamini & Hochberg False
684 Discovery Rate (FDR) multiple testing correction at a significance level of 5%. We
685 chose the 'Biological Process' category and the prokaryotic ontology file
686 (gosubset_prok.obo). However, as most groups did not show significant
687 overrepresentation, we visualized all the GO categories of genes under positive
688 selection and used REVIGO[67] with the p-values from BiNGO in order to obtain
689 summaries of non-redundant GO terms classified into functional categories.
690
691 **Analysis of lactose fermentation.** *S. aureus* was cultured in Tryptic Soy Broth (TSB)
692 in presence or absence of 100 mM lactose at 37°C for 17 h with shaking at 200 rpm.
693 OD_{600} was measured and culture supernatants were collected by centrifugation.
694 Subsequently, the pH of the supernatants was measured using a pH meter (Sartorius,
695 UK). Delta pH values were calculated by subtracting the pH values of TSB cultures
696 supplemented with 100 mM lactose from the pH values of normal TSB cultures.
697 Statistical analysis was performed in Graphpad Prism 7 using One-Way ANOVA
698 followed by Tukey's multiple comparison test.
699
700 **Data availability.** The sequence datasets generated during the current study are
701 available in the European Nucleotide Archive (ENA) (www.ebi.ac.uk/ena) with the

accession number PRJEB20741. Accession numbers of previously published sequences analyzed in the current study are listed in Supplementary Table 1. All data analysed during this study are included in this published article (and its supplementary information files).

References

1. Morand, S., McIntyre, K.M. & Baylis, M. Domesticated animals and human infectious diseases of zoonotic origins: domestication time matters. *Infect Genet Evol* **24**, 76-81 (2014).
2. Woolhouse, M.E., Haydon, D.T. & Antia, R. Emerging pathogens: the epidemiology and evolution of species jumps. *Trends Ecol Evol* **20**, 238-44 (2005).
3. Lowy, F.D. Staphylococcus aureus Infections. *New England Journal of Medicine* **339**, 520-532 (1998).
4. Chambers, H.F. & Deleo, F.R. Waves of resistance: Staphylococcus aureus in the antibiotic era. *Nat Rev Microbiol* **7**, 629-41 (2009).
5. Peton, V. & Le Loir, Y. Staphylococcus aureus in veterinary medicine. *Infect Genet Evol* **21**, 602-15 (2014).
6. Bradley, A.J., Leach, K.A., Breen, J.E., Green, L.E. & Green, M.J. Survey of the incidence and aetiology of mastitis on dairy farms in England and Wales. *Vet Rec* **160**, 253-7 (2007).
7. McNamee, P.T. & Smyth, J.A. Bacterial chondronecrosis with osteomyelitis ('femoral head necrosis') of broiler chickens: a review. *Avian Pathol* **29**, 477-95 (2000).
8. van Duijkeren, E. *et al.* Methicillin-resistant Staphylococcus aureus in pigs with exudative epidermitis. *Emerg Infect Dis* **13**, 1408-10 (2007).
9. Viana, D. *et al.* A single natural nucleotide mutation alters bacterial pathogen host tropism. *Nat Genet* **47**, 361-6 (2015).
10. Feil, E.J. *et al.* How clonal is Staphylococcus aureus? *J Bacteriol* **185**, 3307-16 (2003).
11. Shepheard, M.A. *et al.* Historical zoonoses and other changes in host tropism of Staphylococcus aureus, identified by phylogenetic analysis of a population dataset. *PLoS One* **8**, e62369 (2013).
12. Weinert, L.A. *et al.* Molecular dating of human-to-bovid host jumps by Staphylococcus aureus reveals an association with the spread of domestication. *Biol Lett* **8**, 829-32 (2012).
13. Price, L.B. *et al.* Staphylococcus aureus CC398: host adaptation and emergence of methicillin resistance in livestock. *mBio* **3**(2012).
14. Fitzgerald, J.R. Livestock-associated Staphylococcus aureus: origin, evolution and public health threat. *Trends Microbiol* **20**, 192-8 (2012).
15. Holden, M.T. *et al.* A genomic portrait of the emergence, evolution, and global spread of a methicillin-resistant Staphylococcus aureus pandemic. *Genome Res* **23**, 653-64 (2013).
16. McAdam, P.R. *et al.* Molecular tracing of the emergence, adaptation, and transmission of hospital-associated methicillin-resistant Staphylococcus aureus. *Proc Natl Acad Sci U S A* **109**, 9107-12 (2012).

17. Spoor, L.E. *et al.* Livestock origin for a human pandemic clone of community-associated methicillin-resistant Staphylococcus aureus. *MBio* **4**(2013).
18. Lowder, B.V. *et al.* Recent human-to-poultry host jump, adaptation, and pandemic spread of Staphylococcus aureus. *Proc Natl Acad Sci U S A* **106**, 19545-50 (2009).
19. Viana, D. *et al.* Adaptation of Staphylococcus aureus to ruminant and equine hosts involves SaPI-carried variants of von Willebrand factor-binding protein. *Mol Microbiol* **77**, 1583-94 (2010).
20. Guinane, C.M. *et al.* Evolutionary genomics of Staphylococcus aureus reveals insights into the origin and molecular basis of ruminant host adaptation. *Genome Biol Evol* **2**, 454-66 (2010).
21. Koymans, K.J., Vrieling, M., Gorham, R.D., Jr. & van Strijp, J.A. Staphylococcal Immune Evasion Proteins: Structure, Function, and Host Adaptation. *Curr Top Microbiol Immunol* (2016).
22. Koop, G. *et al.* Identification of LukPQ, a novel, equid-adapted leukocidin of Staphylococcus aureus. *Sci Rep* **7**, 40660 (2017).
23. Loffler, B. *et al.* Staphylococcus aureus panton-valentine leukocidin is a very potent cytotoxic factor for human neutrophils. *PLoS Pathog* **6**, e1000715 (2010).
24. Vrieling, M. *et al.* LukMF' is the major secreted leukocidin of bovine Staphylococcus aureus and is produced in vivo during bovine mastitis. *Sci Rep* **6**, 37759 (2016).
25. de Jong, N.W.M. *et al.* Identification of a staphylococcal complement inhibitor with broad host specificity in equid Staphylococcus aureus strains. *J Biol Chem* **293**, 4468-4477 (2018).
26. Wilson, G.J. *et al.* A novel core genome-encoded superantigen contributes to lethality of community-associated MRSA necrotizing pneumonia. *PLoS Pathog* **7**, e1002271 (2011).
27. Tong, S.Y. *et al.* Novel staphylococcal species that form part of a Staphylococcus aureus-related complex: the non-pigmented Staphylococcus argenteus sp. nov. and the non-human primate-associated Staphylococcus schweitzeri sp. nov. *Int J Syst Evol Microbiol* **65**, 15-22 (2015).
28. Thaipadungpanit, J. *et al.* Clinical and molecular epidemiology of Staphylococcus argenteus infections in Thailand. *J Clin Microbiol* **53**, 1005-8 (2015).
29. Aanensen, D.M. *et al.* Whole-Genome Sequencing for Routine Pathogen Surveillance in Public Health: a Population Snapshot of Invasive Staphylococcus aureus in Europe. *MBio* **7**(2016).
30. Minin, V.N. & Suchard, M.A. Counting labeled transitions in continuous-time Markov models of evolution. *J Math Biol* **56**, 391-412 (2008).
31. De Maio, N., Wu, C.H., O'Reilly, K.M. & Wilson, D. New Routes to Phylogeography: A Bayesian Structured Coalescent Approximation. *PLoS Genet* **11**, e1005421 (2015).
32. Sheppard, S.K. *et al.* Cryptic ecology among host generalist Campylobacter jejuni in domestic animals. *Mol Ecol* **23**, 2442-51 (2014).
33. Deringer, J.R., Ely, R.J., Monday, S.R., Stauffacher, C.V. & Bohach, G.A. Vbeta-dependent stimulation of bovine and human T cells by host-specific staphylococcal enterotoxins. *Infect Immun* **65**, 4048-54 (1997).
34. Howden, B.P., Peleg, A.Y. & Stinear, T.P. The evolution of vancomycin intermediate Staphylococcus aureus (VISA) and heterogenous-VISA. *Infect Genet Evol* **21**, 575-82 (2014).
35. Directorate, P.H.E.a.V.M. UK One Health report: antibiotics use in humans and animals. (2015).
36. Ward, M.J. *et al.* Time-scaled evolutionary analysis of the transmission and antibiotic resistance dynamics of Staphylococcus aureus CC398. *Appl Environ Microbiol* (2014).
37. Murray, S. *et al.* Recombination-Mediated Host Adaptation by Avian Staphylococcus aureus. *Genome Biol Evol* **9**, 830-842 (2017).

38. Ward, M.J. *et al.* Identification of source and sink populations for the emergence and global spread of the East-Asia clone of community-associated MRSA. *Genome Biol* **17**, 160 (2016).
39. Argimon, S. *et al.* Microreact: visualizing and sharing data for genomic epidemiology and phylogeography. *Microb Genom* **2**, e000093 (2016).
40. Zerbino, D.R. Using the Velvet de novo assembler for short-read sequencing technologies. *Curr Protoc Bioinformatics* **Chapter 11**, Unit 11 5 (2010).
41. Zerbino, D.R. & Birney, E. Velvet: algorithms for de novo short read assembly using de Bruijn graphs. *Genome Res* **18**, 821-9 (2008).
42. Boetzer, M., Henkel, C.V., Jansen, H.J., Butler, D. & Pirovano, W. Scaffolding pre-assembled contigs using SSPACE. *Bioinformatics* **27**, 578-9 (2011).
43. Nadalin, F., Vezzi, F. & Policriti, A. GapFiller: a de novo assembly approach to fill the gap within paired reads. *BMC Bioinformatics* **13 Suppl 14**, S8 (2012).
44. Li, H. *et al.* The Sequence Alignment/Map format and SAMtools. *Bioinformatics* **25**, 2078-9 (2009).
45. Stamatakis, A. RAxML version 8: a tool for phylogenetic analysis and post-analysis of large phylogenies. *Bioinformatics* **30**, 1312-3 (2014).
46. Drummond, A.J., Suchard, M.A., Xie, D. & Rambaut, A. Bayesian phylogenetics with BEAUti and the BEAST 1.7. *Mol Biol Evol* **29**, 1969-73 (2012).
47. Ayres, D.L. *et al.* BEAGLE: an application programming interface and high-performance computing library for statistical phylogenetics. *Syst Biol* **61**, 170-3 (2012).
48. Seemann, T. Prokka: rapid prokaryotic genome annotation. *Bioinformatics* **30**, 2068-9 (2014).
49. Camacho, C. *et al.* BLAST+: architecture and applications. *BMC Bioinformatics* **10**, 421 (2009).
50. Jones, P. *et al.* InterProScan 5: genome-scale protein function classification. *Bioinformatics* **30**, 1236-40 (2014).
51. Aibar, S., Fontanillo, C., Droste, C. & De Las Rivas, J. Functional Gene Networks: R/Bioc package to generate and analyse gene networks derived from functional enrichment and clustering. *Bioinformatics* **31**, 1686-8 (2015).
52. Delcher, A.L., Phillippy, A., Carlton, J. & Salzberg, S.L. Fast algorithms for large-scale genome alignment and comparison. *Nucleic Acids Res* **30**, 2478-83 (2002).
53. Contreras-Moreira, B. & Vinuesa, P. GET_HOMOLOGUES, a versatile software package for scalable and robust microbial pangenome analysis. *Appl Environ Microbiol* **79**, 7696-701 (2013).
54. Rice, P., Longden, I. & Bleasby, A. EMBOSS: the European Molecular Biology Open Software Suite. *Trends Genet* **16**, 276-7 (2000).
55. Wright, D.W., Angus, T., Enright, A.J. & Freeman, T.C. Visualisation of BioPAX Networks using BioLayout Express (3D). *F1000Res* **3**, 246 (2014).
56. Paradis, E. Analysis of diversification: combining phylogenetic and taxonomic data. *Proc Biol Sci* **270**, 2499-505 (2003).
57. David, S. *et al.* Evaluation of an Optimal Epidemiological Typing Scheme for Legionella pneumophila with Whole-Genome Sequence Data Using Validation Guidelines. *J Clin Microbiol* **54**, 2135-48 (2016).
58. Barker, D., Meade, A. & Pagel, M. Constrained models of evolution lead to improved prediction of functional linkage from correlated gain and loss of genes. *Bioinformatics* **23**, 14-20 (2007).
59. Rambaut A, S.M., Xie D, and Drummond AJ. Tracer v 1.6. (2014).
60. Edgar, R.C. MUSCLE: multiple sequence alignment with high accuracy and high throughput. *Nucleic Acids Res* **32**, 1792-7 (2004).

61. Suyama, M., Torrents, D. & Bork, P. PAL2NAL: robust conversion of protein sequence alignments into the corresponding codon alignments. *Nucleic Acids Res* **34**, W609-12 (2006).
62. Bruen, T., Bruen, T. PhiPack: PHI test and other tests of recombination. (McGill University, Montreal, Quebec, 2005).
63. Huerta-Cepas, J., Serra, F. & Bork, P. ETE 3: Reconstruction, Analysis, and Visualization of Phylogenomic Data. *Mol Biol Evol* **33**, 1635-8 (2016).
64. Yang, Z. PAML 4: phylogenetic analysis by maximum likelihood. *Mol Biol Evol* **24**, 1586-91 (2007).
65. Zhang, J., Nielsen, R. & Yang, Z. Evaluation of an improved branch-site likelihood method for detecting positive selection at the molecular level. *Mol Biol Evol* **22**, 2472-9 (2005).
66. Maere, S., Heymans, K. & Kuiper, M. BiNGO: a Cytoscape plugin to assess overrepresentation of gene ontology categories in biological networks. *Bioinformatics* **21**, 3448-9 (2005).
67. Supek, F., Bosnjak, M., Skunca, N. & Smuc, T. REVIGO summarizes and visualizes long lists of gene ontology terms. *PLoS One* **6**, e21800 (2011).
68. Reuter, S. *et al.* Building a genomic framework for prospective MRSA surveillance in the United Kingdom and the Republic of Ireland. *Genome Res* (2015).

Acknowledgments

The study was supported by a project grant (BB/K00638X/1) and institute strategic grant funding ISP2: BB/P013740/1 from the Biotechnology and Biological Sciences Research Council (UK) to J.R.F, Medical Research Council (UK) grant MRNO2995X/1 to J.R.F. and Wellcome Trust collaborative award 201531/Z/16/Z to J.R.F. S.Y.C.T. is an Australian National Health and Medical Research Council Career Development Fellow (#1065736). L.A.W is supported by a Dorothy Hodgkin Fellowship funded by the Royal Society (Grant Number DH140195) and a Sir Henry Dale Fellowship jointly funded by the Wellcome Trust and the Royal Society (Grant Number 109385/Z/15/Z). S.L. is supported by a Chancellor's Fellowship from the University of Edinburgh. M.T.G.H was supported by the Scottish Infection Research Network and Chief Scientist Office through the Scottish Healthcare Associated Infection Prevention Institute consortium funding (CSO Reference: SIRN10). E.M.H. and S.J.P were funded by The Health Innovation Challenge Fund (WT098600, HICF-T5-342), a parallel funding partnership between the Department of Health and Wellcome Trust, and the UKCRC Translational Infection Research Initiative, and the Medical Research Council (Grant Number G1000803). S.J.P. is a National Institute for Health Research Senior Investigator.

M.T.G.H was supported by the Scottish Infection Research Network and Chief Scientist Office through the Scottish Healthcare Associated Infection Prevention Institute consortium funding (CSO Reference: SIRN10) M.T.G.H was supported by the Scottish Infection Research Network and Chief Scientist Office through the Scottish Healthcare Associated Infection Prevention Institute consortium funding (CSO Reference: SIRN10). P.A.H. is supported by Natural Environment Research Council for Grant NE/M001415/1. We thank Beth Blane, Nick Brown and Estee Torok for their role in the original study that isolated and sequenced *S. aureus* from patients at the Cambridge University Hospitals NHS Foundation Trust [68], from which 76 genomes were downloaded from the ENA and used in this study. We also thank Edinburgh Genomics for sequencing, and all those who made isolates available for the study including Zoological Society London, G. Foster, H. Hasman, S. Monecke, E. Smith, D. Smyth, and H. Jorgensen.

Author contributions

J.R.F. S.J.P, J.P, M.H., E.M.H, L.A.W., and M.T.G.H., conceived and designed the study. E.J.R., R.B., E.M.H., L.A.W., S.L , M.V. and K.R. carried out experiments. E.J.R., R.B., E.M.H., L.A.W., S.L., G.K.P, D.M.A., M.T.H., E.J.F., J.C., M.V., P.A.H., K.R. and J.R.F analysed data. S.Y.C.T., A.S., and W.vW. provided isolates. E.J.R., R.B., E.M.H., S.L. and J.R.F. wrote the manuscript. All authors contributed to manuscript editing.

Competing Interests

The authors declare no competing interests.

Figure legends

Figure 1. ***Staphylococcus aureus*** **phylogeny according to host-species origin**. (a) Phylogenetic tree of 800 isolates constructed using the maximum liklihood (ML) method demonstrating the relationship between *S. aureus* and other members of the *S. aureus* complex; *S. schweitzeri* and *S. argenteus*; (b) Phylogenetic (ML) tree of 783 *S. aureus* isolates, with host species indicated in colour or animal symbols indicating major

domesticated animal clones that are largely host-specific. The evolutionary history of *S. aureus* was calibrated using well-established substitution rates from published datasets (see methods).

Figure 2. *S. aureus* has undergone extensive ancient and recent host-switching events with humans acting as a major hub. (a) Time-scaled phylogeny of a subsample of the *S. aureus* sequences with clonal complexes (CCs) labeled, branches colored according to host-species group. Pie charts indicate relative probability of host origin at the ancestral nodes, and line thickness corresponds to probability of the majority host (see Supplementary Figures 6-10 for all subsamples). Major clonal complexes (CC)s are indicated. (b) Quantification of the number of host-switch events: Host transition count network from BEAST Markov Jumps models averaged over all subsamples of the data. Line-width represents the average Markov Jump count per tree, averaged over all subsamples (Supplementary Figures 4-5) and line color represents the significance compared to permuted label analysis (Z-score). Only transitions with higher counts compared to models with permuted host-labels are shown (Z-score >= 0.5).

Figure 3. Network analysis of *S. aureus* accessory genome indicates clustering according to host species group. Network graph of pairwise distances of accessory genome gene content between isolates. Each node represents an isolate, colour-coded to indicate host species origin, and each edge indicates greater than 50% of shared accessory genome content with the length of the edges weighted by distance (proportion of shared accessory genes; shorter edges have more genes in common). All edges with <50% shared accessory genome content were removed.

Figure 4. Identification of horizontally-acquired genetic elements correlated with host-adaptation. (a) Schematic representation of the *S. aureus* pan-genome with gene clusters linked to host-species indicated by shading. Coloured symbols indicate the nature of the mobile genetic element and the associated host-species (b) Annotated gene maps of selected novel genetic elements linked to specific host species.

associated with acquisition of MGEs from an accessory gene pool that exists in the recipient host-species, and/or loss of MGEs linked to the source species.

Figure 5. Summary of biological pathways under positive selection in different host-species and evidence for phenotypic adaptation. The main anatomical isolation sites on each host group are indicated by filled circles. Functional categories *virulence and pathogenesis*, *resistance to antibiotics*, *transport of ions* and *cell wall biosynthesis* were under positive selection in all 4 host-species groups. In humans (a) and ruminants (b) the categories *amino acids biosynthesis* and *transport/metabolism of carbohydrates* were positively selected. The categories *amino-acid transport/metabolism* and *biosynthesis of osmoprotectants* were under positive selection in birds (c) and *transposable elements* in pigs (d). (e) Phylogenetic tree indicating the distinct lineages selected for comparative analysis of lactose fermentation,(f) Fermentation of the disaccharide lactose is enhanced in bovine lineages. Acidification of *S. aureus* culture supernatant in presence of 100 mM lactose as indicated by the delta pH. Experiments were performed in triplicate with 5 strains per clonal lineage. Each dot represents the average delta pH per strain and bars indicate the SEM per clonal lineage (n = 5). Asterisks indicate significant differences between bovine (CC97 and CC151, n = 10), avian (CC5 and CC385, n = 10) and human lineages (CC22, CC30, and CC8, n = 15) with **P<0.005, ***P<0.001 and ****P<0.0001 using One-Way ANOVA followed by Tukey's multiple comparison test.

Figure 6. Resistance to antimicrobials is non-randomly associated with host species. Proportion (%) of isolates examined which contain the specified resistance determinant (Supplementary Table 12). Asterisks indicate significant association of resistance determinants with host-species (Fisher exact test), and colored borders indicate antibiotic class or single determinants (*sdrM* and *str*) that are associated with host-species group after testing for phylogenetic independence.

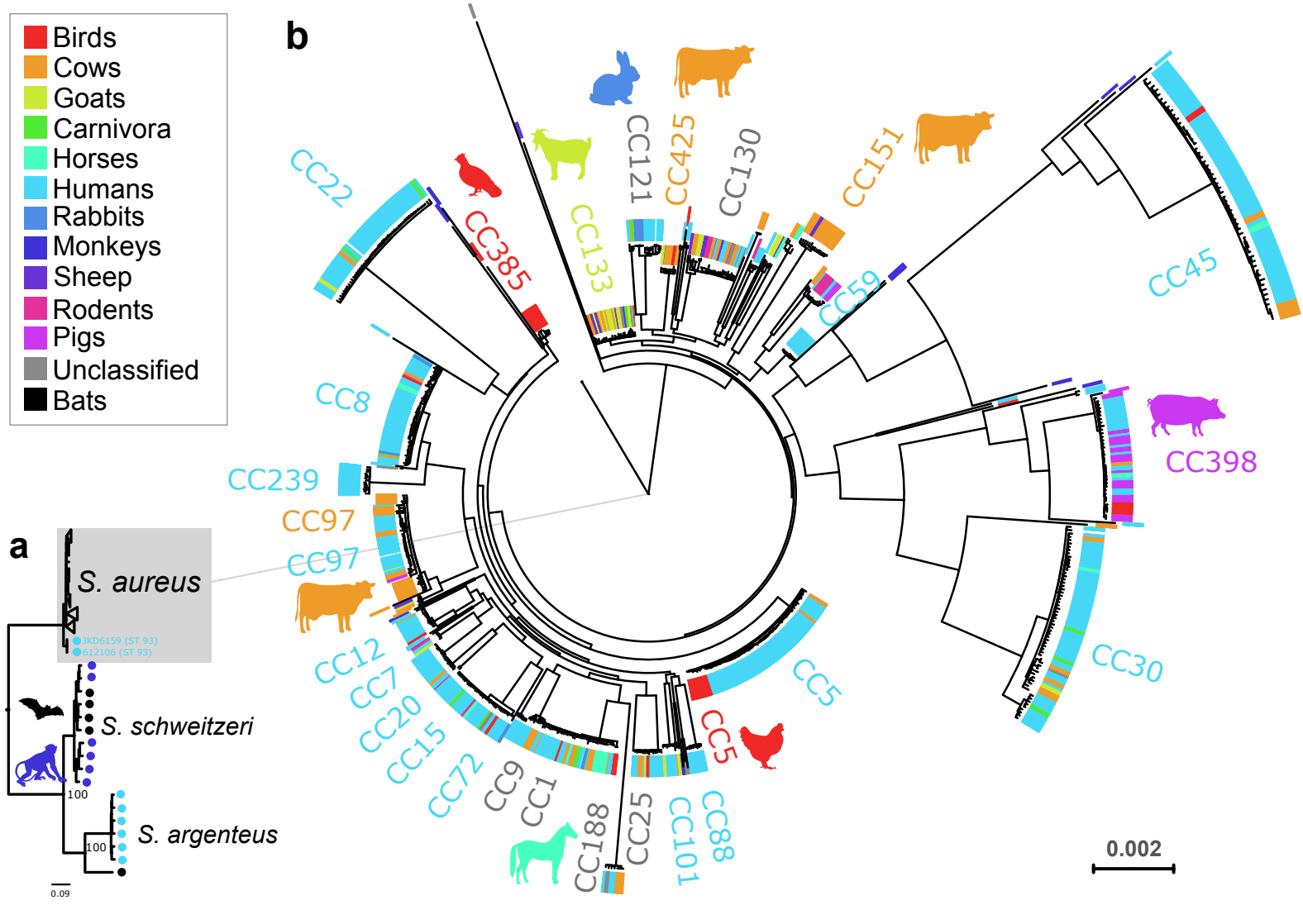
Birds
Cows
Goats
Carnivora
Horses
Humans
Rabbits
Monkeys
Sheep
Rodents
Pigs
Unclassified
Bats
a
S. aureus
JKD6159 (ST 93)
612106 (ST 93)
S. schweitzeri
S. argenteus
100
100
0.09
b
CC22
CC385
CC121
CC425
CC130
CC151
CC133
CC59
CC45
CC8
CC239
CC398
CC97
CC97
CC12
CC7
CC20
CC15
CC72
CC9
CC1
CC188
CC25
CC101
CC88
CC5
CC5
CC30
0.002

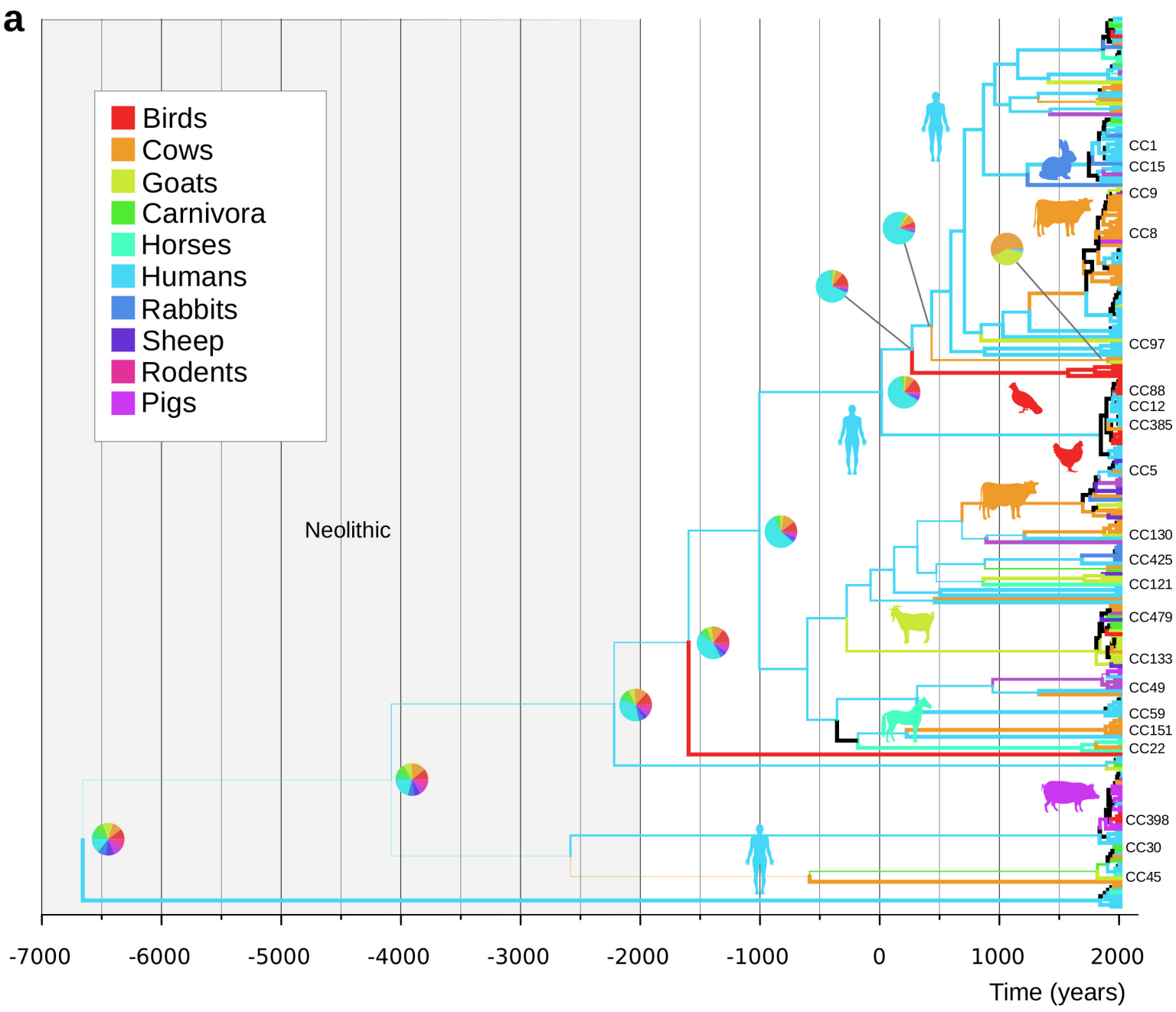
a
Birds
Cows
Goats
Carnivora
Horses
Humans
Rabbits
Sheep
Rodents
Pigs
Neolithic
CC1
CC15
CC9
CC8
CC97
CC88
CC12
CC385
CC5
CC130
CC425
CC121
CC479
CC133
CC49
CC59
CC151
CC22
CC398
CC30
CC45
-7000
-6000
-5000
-4000
-3000
-2000
-1000
0
1000
2000
Time (years)

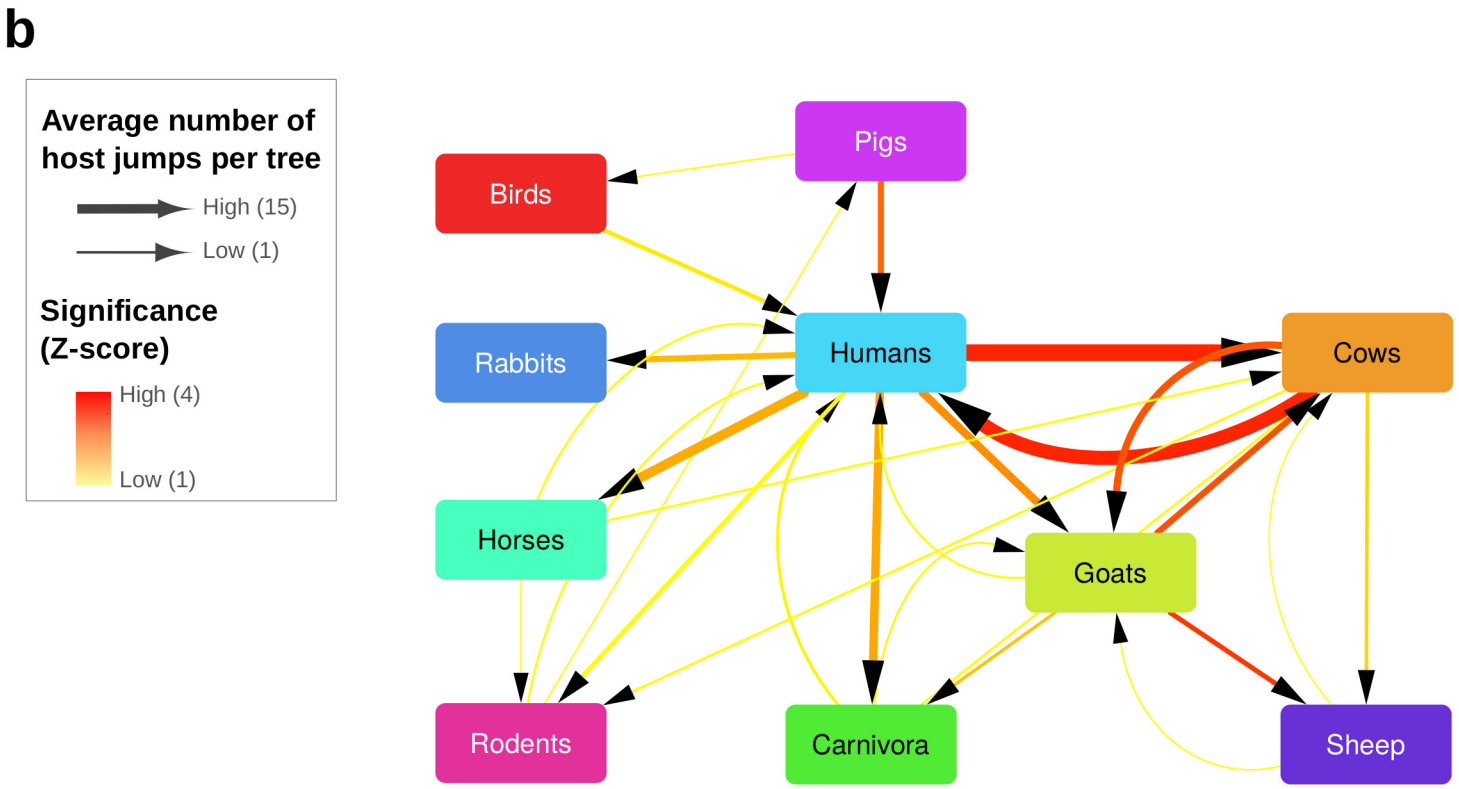
b
Average number of host jumps per tree
High (15)
Low (1)
Significance (Z-score)
High (4)
Low (1)
Pigs
Birds
Rabbits
Humans
Cows
Horses
Goats
Rodents
Carnivora
Sheep

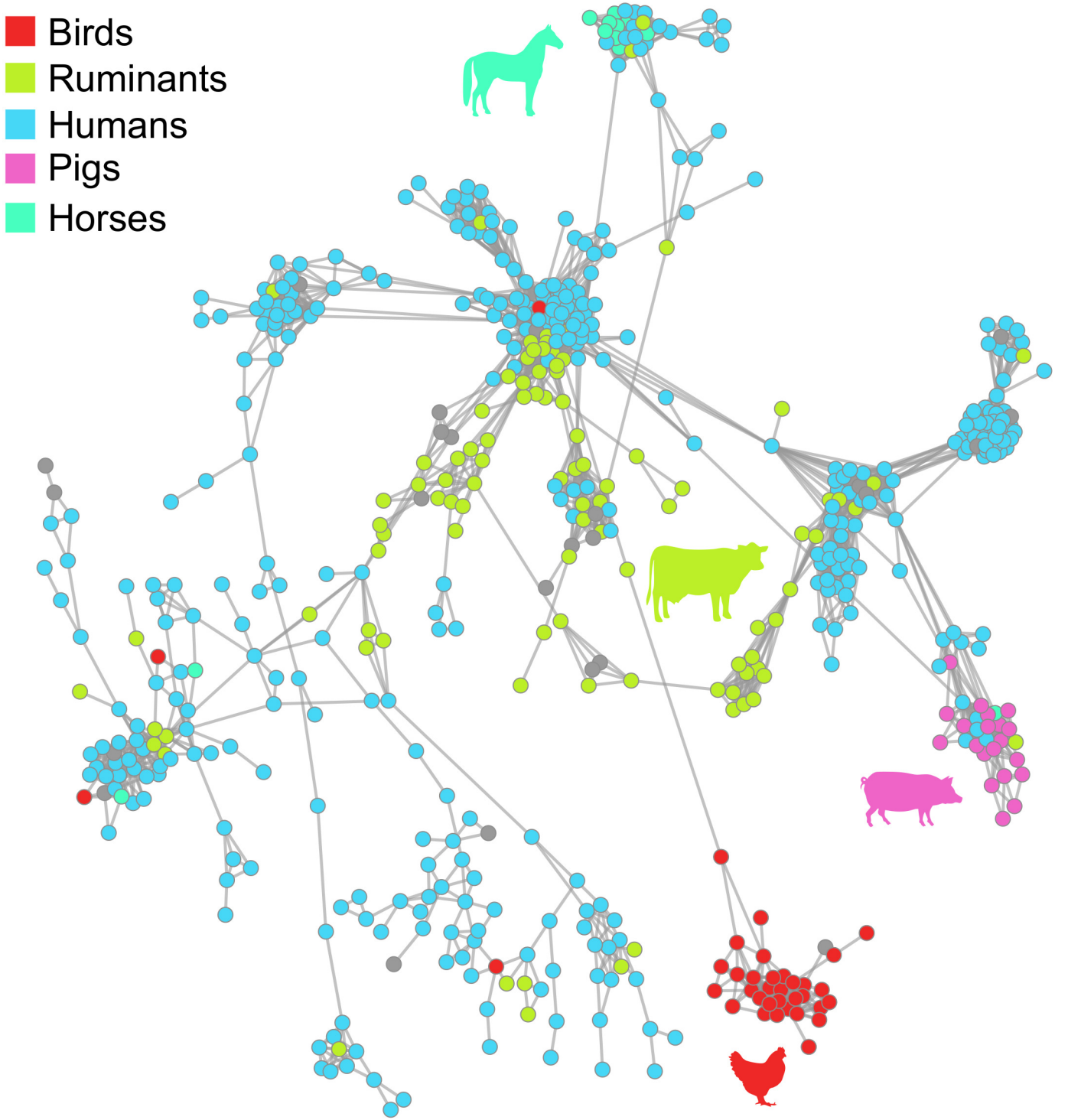
Birds
Ruminants
Humans
Pigs
Horses

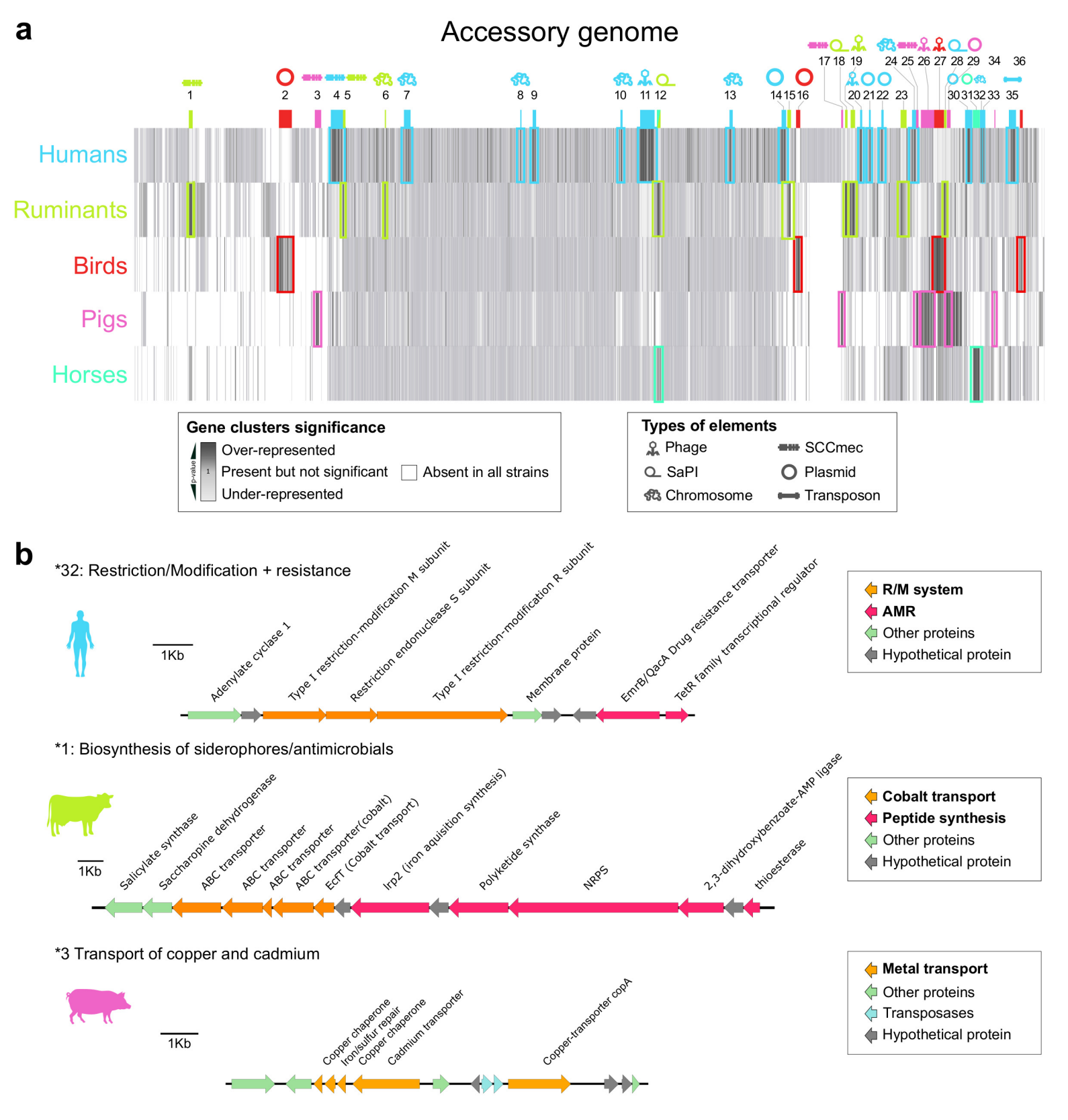
a
Accessory genome
1
2
3
4 5
6
7
8 9
10
11 12
13
14 15 16
17 18 19
20 21 22
23
24 25 26 27
28 29
30 31 32
33
34
35
36
Humans
Ruminants
Birds
Pigs
Horses
Gene clusters significance
Over-represented
Present but not significant
Under-represented
Absent in all strains
p-value
Types of elements
Phage
SaPI
Chromosome
SCCmec
Plasmid
Transposon
b
*32: Restriction/Modification + resistance
1Kb
Adenylate cyclase 1
Type I restriction-modification M subunit
Restriction endonuclease S subunit
Type I restriction-modification R subunit
Membrane protein
EmrB/QacA Drug resistance transporter
TetR family transcriptional regulator
R/M system
AMR
Other proteins
Hypothetical protein
*1: Biosynthesis of siderophores/antimicrobials
1Kb
Salicylate synthase
Saccharopine dehydrogenase
ABC transporter
ABC transporter
ABC transporter
ABC transporter(cobalt)
EcfT (Cobalt transport)
Irp2 (iron aquisition synthesis)
Polyketide synthase
NRPS
2,3-dihydroxybenzoate-AMP ligase
thioesterase
Cobalt transport
Peptide synthesis
Other proteins
Hypothetical protein
*3 Transport of copper and cadmium
1Kb
Copper chaperone
Iron/sulfur repair
Copper chaperone
Cadmium transporter
Copper-transporter copA
Metal transport
Other proteins
Transposases
Hypothetical protein

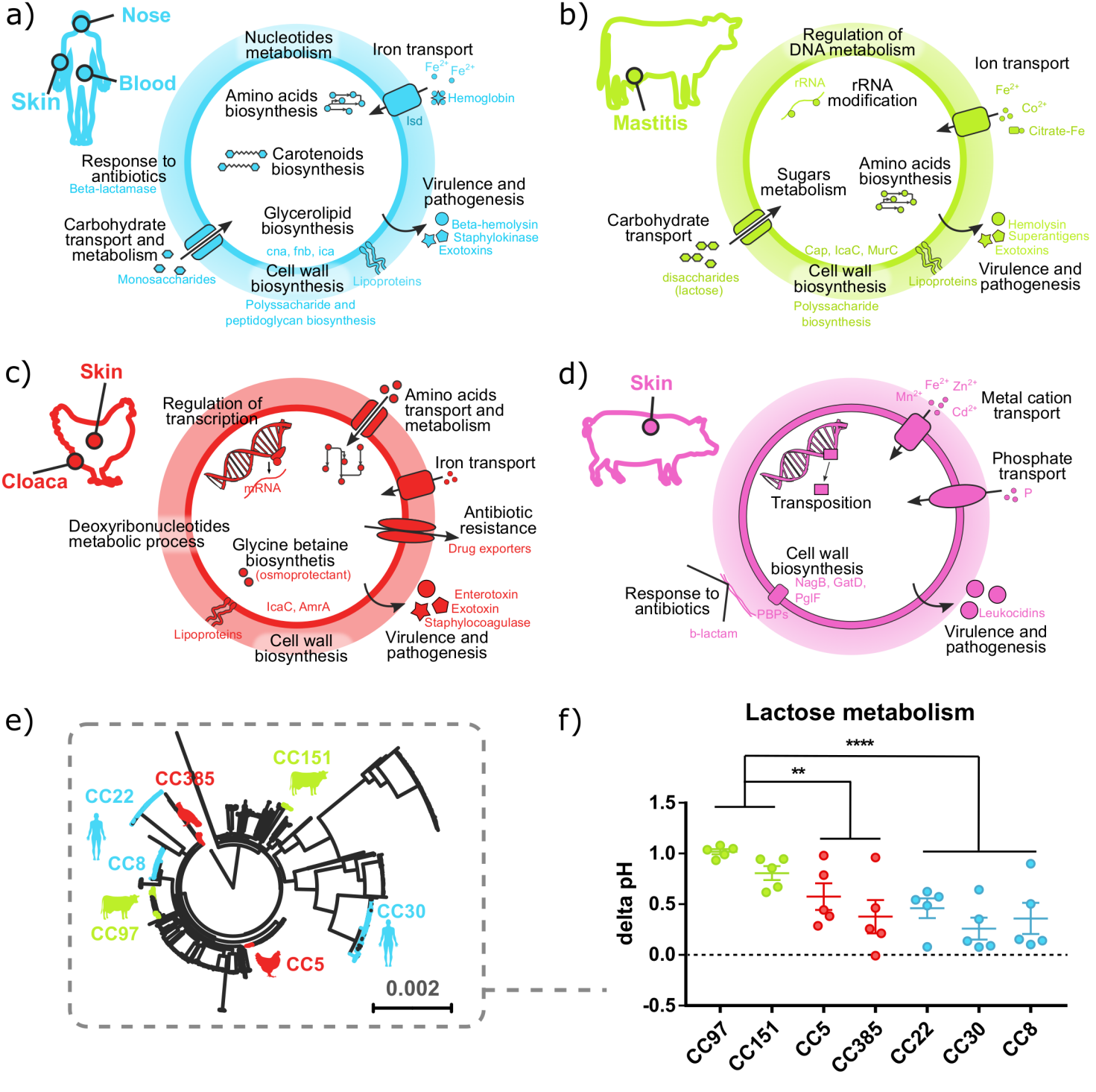
a)
Nose
Skin
Blood
Nucleotides metabolism
Iron transport
Fe2+ Fe2+
Hemoglobin
Isd
Amino acids biosynthesis
Carotenoids biosynthesis
Response to antibiotics
Beta-lactamase
Virulence and pathogenesis
Beta-hemolysin
Staphylokinase
Exotoxins
Glycerolipid biosynthesis
cna, fnb, ica
Carbohydrate transport and metabolism
Monosaccharides
Cell wall biosynthesis
Lipoproteins
Polyssacharide and peptidoglycan biosynthesis
b)
Mastitis
Regulation of DNA metabolism
Ion transport
rRNA
rRNA modification
Fe2+
Co2+
Citrate-Fe
Sugars metabolism
Amino acids biosynthesis
Carbohydrate transport
disaccharides (lactose)
Hemolysin
Superantigens
Exotoxins
Cap, IcaC, MurC
Cell wall biosynthesis
Lipoproteins
Virulence and pathogenesis
Polyssacharide biosynthesis
c)
Skin
Cloaca
Regulation of transcription
mRNA
Amino acids transport and metabolism
Iron transport
Antibiotic resistance
Drug exporters
Deoxyribonucleotides metabolic process
Glycine betaine biosynthetis
(osmoprotectant)
IcaC, AmrA
Enterotoxin
Exotoxin
Staphylocoagulase
Lipoproteins
Cell wall biosynthesis
Virulence and pathogenesis
d)
Skin
Fe2+ Zn2+
Mn2+
Cd2+
Metal cation transport
Phosphate transport
P
Transposition
Cell wall biosynthesis
NagB, GatD, PglF
Response to antibiotics
PBPs
b-lactam
Leukocidins
Virulence and pathogenesis
e)
CC151
CC385
CC22
CC8
CC97
CC30
CC5
0.002
f)
Lactose metabolism
****
**
delta pH
1.5
1.0
0.5
0.0
-0.5
CC97
CC151
CC5
CC385
CC22
CC30
CC8

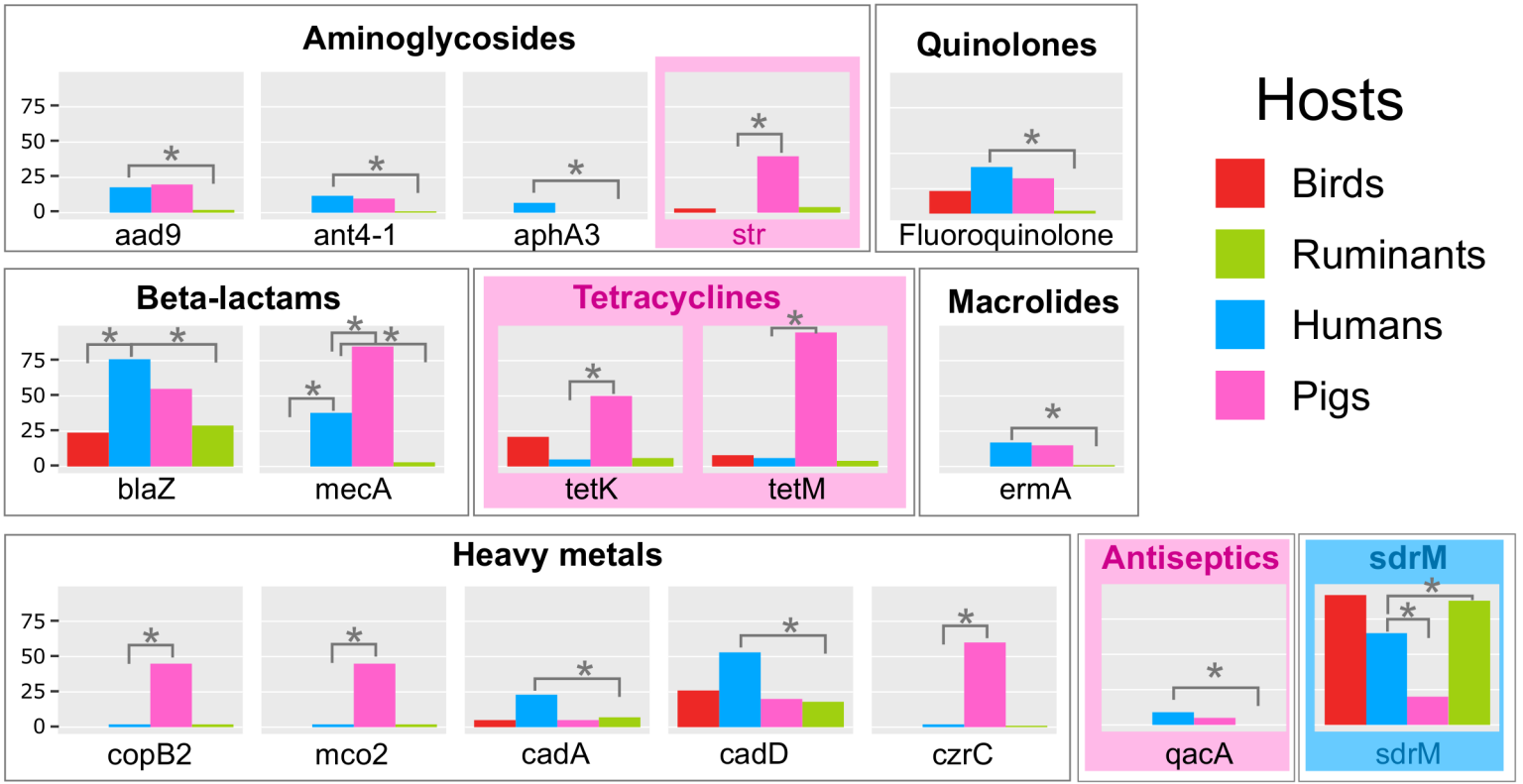
Aminoglycosides
75
50
25
0
aad9
ant4-1
aphA3
str
Quinolones
Fluoroquinolone
Beta-lactams
blaZ
mecA
Tetracyclines
tetK
tetM
Macrolides
ermA
Heavy metals
copB2
mco2
cadA
cadD
czrC
Antiseptics
qacA
sdrM
sdrM
Hosts
Birds
Ruminants
Humans
Pigs